water

MDPI

Article

Geomorphic Effects of a Dammed Pleistocene Lake Formed by Landslides along the Upper Yellow River

Xiaohua Guo [1,*], Jiuchuan Wei [1], Yudong Lu [2], Zhaojun Song [1] and Huimin Liu [1]

[1] College of Earth Science and Engineering, Shandong University of Science and Technology, Qingdao 266590, China; jcwee@126.com (J.W.); songzhaojun76@163.com (Z.S.); Lhuimin91@163.com (H.L.)

[2] Key Laboratory of Subsurface Hydrology and Ecological Effect in Arid Region of Ministry of Education, School of Environmental Science and Engineering, Chang'an University, Xi'an 710064, China; luyudong@chd.edu.cn

* Correspondence: skd996039@sdust.edu.cn

Received: 21 April 2020; Accepted: 6 May 2020; Published: 9 May 2020

Abstract: In a previous study two pairs of paleo-landslides within an 8 km reach of the upper Yellow River were studied and dated back to ca. 80 ka, however the relationship between these two pairs of paleo-landslides were not explored. This study inferred that the initial pair of landslides (Dehenglong and Suozi) appearing contiguously and forming an upstream 46 km-long lake along the river may be triggered by earthquake events from nearby capable faults. Subsequently, backwater inundating the valley floor as the dammed lake formed may cause shear stress of sediments lowered on steep slopes adjacent to the River, and eventually induce the other two additional landslides (Xiazangtan and Kangyang) ~8 km upstream. This could be inferred from two optically stimulated luminescence (OSL) samples yielding ca. 80 ka also, which were collected from asymmetric folds 10 to 30 cm in amplitude within the bedding plane between lake/lakeshore sediment and landslide mass at the front lobes of the two additional landslides. We estimated the maximum volume of this dammed lake was 38 km^3 and may generate an outburst flood with an estimated peak discharge of 6.1×10^5 m^3/s, which may cause massive geomorphic effects and potential disasters upstream and downstream. It is important to better understand the geomorphic process of this damming event in mountainous area with respect to reflecting tectonic uplift, paleoclimatic change and forecast and mitigate hazards on the northeast Tibetan Plateau.

Keywords: landslides-dammed lake; hypothetical flood; DEM; OSL; Upper Yellow River

1. Introduction

Dams formed by ice, moraines, or landslides in particular may be short lived and can give rise to large outburst flows following sudden failure, potentially resulting in substantial loss of life and damage to property [1–3]. Therefore, this topic has received increasing attention in recent years, and systematically studying these naturally formed dammed lakes is of great importance to making mitigation strategies in the future [4–9]. Landslide dams and associated dammed lake deposits may reside in the channel for $>10^4$ years [10–13] and can result in a variety of geomorphic effects of landslides on the landscape and river system. Some geomorphic effects may be much more complex and important due to different magnitudes of the fluvial system or landslide mass body. Landslides damming the upstream of the Yellow River on the northeastern side are significant, not only because of the huge dimensions of the landslides but due to the enormous catchment area impounded by the dam and the recognition that a river as large as the Yellow River has been and can be impacted by a persistent river-blocking landslide. However, most of the dammed lakes along the upper stream of the Yellow River were not systematically studied, including a 46 km-long dammed

lake stretching from Dehenglong and Suozi landslides, which reflects a large gap in the timing and rates of geomorphic and sedimentary processes in China's mountainous areas [14]. This dammed lake has an upstream catchment area of 212.5 km^2 and we believe this to be by far the largest catchment area ever reported for a significant landslide dam on the northeastern Tibetan Plateau. Previous studies had estimated the emplacement timing of Dehenglong and Suozi landslides and dammed lake, respectively, by using optically stimulated luminescence (OSL) methods on quartz grains [15,16]. Lacustrine sediment in a perched lake that formed on the Dehenglong landslide yielded OSL aged 89 ± 8 ka [15,16]. The Suozi landslide was emplaced by rotational slip, which formed dislocation breccias at the basal shear outlet and subsequently dammed the Yellow River [15]. An OSL age on quartz grains from the shattered Triassic gneiss returned 71 ± 6 ka, indicating the Suozi landslide emplaced ca. 71 ka [15]. Twelve OSL ages from the lacustrine sediments returned ca. 80 ka for the dam lake that was formed resultingfrom the failure of Dehenglong and Suozi landslides [17], indicating that the ages of Dehenglong and Suozi landslides and the dammed lake were consistent at two sigma errors [17]. Two adjacent landslides, named Xiazangtan and Kangyang landslides were studied as well, 8 km upstream of the Dehenglong–Suozi landslides. Lacustrine sediments in a perched lake above Xiazangtan landslide yielded an OSL age of 75 ± 9 ka; whereas OSL ages of 33 and 85 ka from loess overlying the landslide and dammed deposits at the front lobe of the landslide provide bounding limiting ages for Kangyang landslide [18,19].

Although the emplace timing for these four landslides has been studied [15,16,20–23], less apparent is the geomorphic imprints of landslide dams on the river and causative factors for these four landslides. There are many aspects of the geomorphic effects of landslide dams on the river system, and this study focuses on the geomorphic effects on the upstream slope and the peak discharge after breaching. It has been reported that downstream of the blockage, backwater inundating the valley floor as a dammed lake formed may increase pore water pressure, consequently inducing upstream secondary slope failures with the risk of displacement waves [24]. It is uncertain whether the failures of Xiazangtan and Kangyang landslides are associated with the downstream blockage caused by the Dehenglong–Suozi landslides. Little is also known about which aspects these four simultaneously emplaced landslides reflect, a heightened period of tectonic activity, excessive precipitation, other allogeneic fluvial processes or a combination of factors. Newly formed dams often induce upstream flooding as the impounded lake level rises, in turn, it may also cause downstream flooding when breached. Dehenglong–Suozi landslides, catastrophic dam failures, may cause huge peak discharge when breached [25], and subsequently induce large-scale erosion with sediment yield magnitudes greater than prior to the dam breach [11,26].

Understanding the spatial distribution, magnitude and peak discharge of the effects of large floods on valley fluvial system is important for determining their long-term geomorphic processes as key agents for shaping the topography of mountain ranges and setting local base level for hillslopes [27,28]. Thus in this study, two stratigraphic sections and two associated OSL ages were studied well to reveal the correlations between the initial and additional pairs of landslides along the Yellow River. The spatial distribution, magnitude and peak discharge were evaluated for the paleolake that inundated the upper Yellow River valley. All this new information is placed in context with previous studies of dam lake and landslides along the Yellow River [15,17,20,22], to further assess the geomorphic effects of landslides and impounded lake sediments along the Yellow River on the northeastern Tibetan Plateau.

2. Sedimentologyand Tectonic Context

This study focused on the landslide record in Jishi Gorge-Songba Gorge along the upper reaches of the Yellow River (35°20′–36°20′ N, 100°15′–103°25′ E; Figure 1) at the junction of eastern Qinghai Province and western Gansu Province; and is at the transition between the Loess Plateau and the Qinghai–Tibetan Plateau. The Yellow River flows across the northeastern Tibetan Plateau with an average altitude of ~4000 m above sea level (m a.s.l.), and descends through a series of Cenozoic basins. This river incised at ~1.1 Ma and formed the Jishi Gorge and the fifth fluvial terrace at 900 m

above the river level (2750 m a.s.l.) in Xunhua Basin [29]. The degradation of the Yellow River initiated sometime ca. 0.13 Ma and incised 800 to 1000 m deep into the bedrock to form the Longyang Gorge, about 80 km to the west of Songba Gorge [29]. Five terrace sequences were recognized at 95 to 15 m above the river level, yielding OSL ages of ca. 79 ± 6, 65.8 ± 5.2, 25.3 ± 2.4, 16.9 ± 1.3, 11.5 ± 1.3 ka in Jianzha Basin [19]. Nine conspicuous terraces (T1–T9) were identified in the Guide Basin that occurred from 5 to 220 m above river level and the current river level is 1980 m a.s.l. The ages of the nine terraces were constrained by thermoluminescence (TL) dating on quartz grains from the lowest (T1) to the highest (T9) terraces at ca. 9, 18, 43, 53, 88, 105, 140, 187 and >187 ka [30]. Deep landscape dissection by the Yellow River and tributaries has resulted in narrow and high-relief river gorges that are sources for landslides on the northeastern Tibetan Plateau.

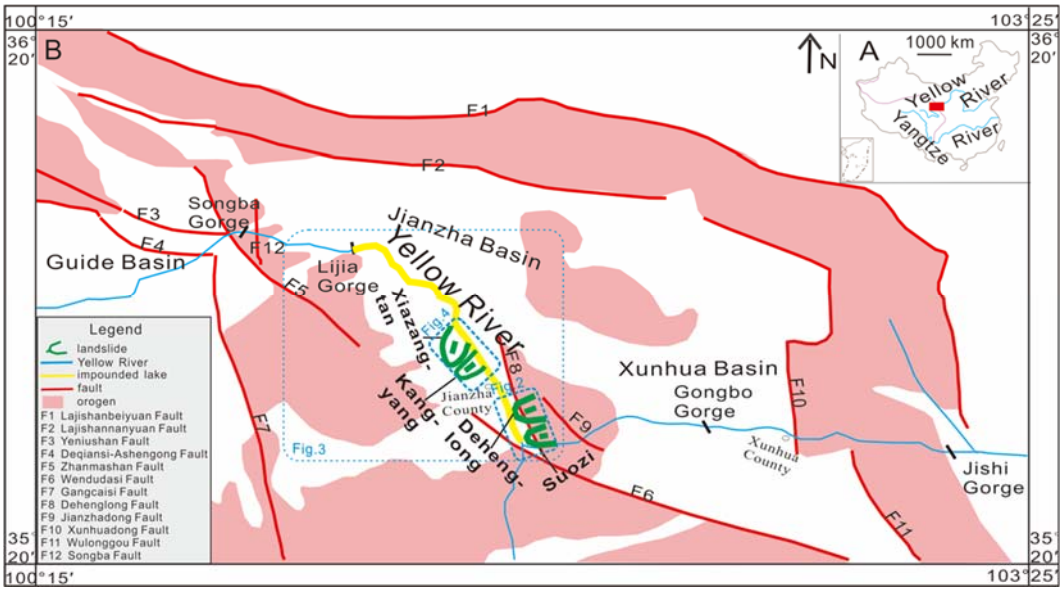

Figure 1. Map showing geographical location of the study area in China. (**A**) The small red rectangle denotes the locations of our study area. (**B**) Distribution of landslides and faults.

The Tibetan Plateau has experienced substantial tectonic uplift since the middle Quaternary, and the upper reaches of the Yellow River has cut deeply (>600 m) into a series of bedrock ranges and intermountain basins [31,32], including Guide, Jianzha and Xunhua basins in the study area. Approximate 12 recognized faults trend northwest to southeast between Songba and Jishi gorges (Figure 1). The Dehenglong and Jianzhadong thrust faults (F8 and F9 in Figure 1B) bound the Qilian Shan-Xi Qinling block and may be epicenters of past earthquakes. Dehenglong and Suozi landslides are in proximity to these two faults (Figure 1). Furthermore, recent seismic data indicate that these two faults are currently active, generating >5 magnitude earthquakes [22,33].

The lithologies of exposed rocks along the gorge are Triassic gneiss and mostly Neogene red mudstones. The climate in the study area is semi-arid, with an annual temperature range between −28 °C and 25 °C, an annual average precipitation of ~342 mm, and an evaporation rate of ~1689 mm. Sedimentary sequences exposed along the upper reaches of the Yellow River, therefore, bear a signature of past interactions between climate and surface processes in the cold and semi-arid regions of the northeastern Tibetan Plateau.

The locations of landslides were identified through analyses of images from the Google Earth portal and were evaluated subsequently with a field survey. A large number of small-scale landslides, about 10,000 m^2 in area, were observed along both banks of the upper reaches of the Yellow River. However, two adjoining paleo-landslides, Dehenglong and Suozi with estimated volumes of 14.35×10^8 m^3 and 21.45×10^8 m^3 [33], respectively were sufficiently large to dam the Yellow River (Figure 2). The head scarps of both landslides appear to emanate near the Jianzhadong Fault

(F9 in Figure 1B) (255°∠48°, strike and dip of fault plane); whereas, the Dehenglong Fault (F8 in Figure 1B) (75°∠65°) appears to emplace the front lobe of the landslides [22]. The landslide deposits were mostly composed of large blocks of Triassic gneiss, which was an erosion-resisting material for damming the Yellow River. The basement rock, from which Dehenglong and Suozi landslides were detached, was a Neogene red mudstone overlain by Triassic gneiss. Opposite the Dehenglong and Suozi landslides, on the south bank of the Yellow River, numerous 1–2 m-wide blocks of Triassic gneiss were observed; the same material that composed the landslide mass on the north river bank. These geomorphic relations indicate that the blocks of Triassic gneiss in Dehenglong and Suozi landslides were transported across the Yellow River and dammed the river flow [16]. These two adjacent landslides appeared to co-occur with a common lateral boundary and geomorphic position and, thus, we inferred that the combined Dehenglong-Suozi landslides dammed the Yellow River forming a large lake behind the landslide mass [16].

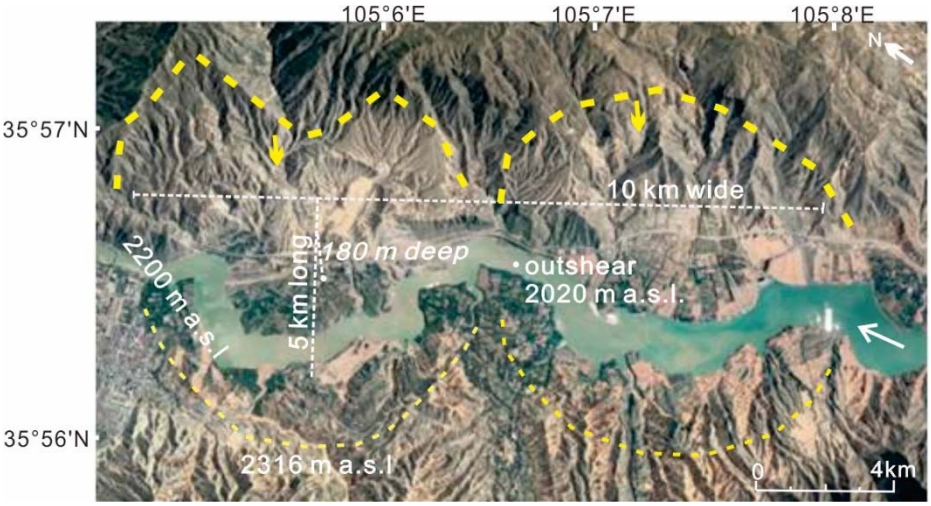

Figure 2. The scale of the Dehenglong–Suozi landslides dam from Google images. Yellow dashed curves indicate the extents of the landslides. Yellow arrows represent the source of landslide. White arrow denotes the flow direction of the Yellow River. "2316 m a.s.l." denotes the run-up height elevation of Dehenglong–Suozi landslides on the west side of river. "2200 m a.s.l." denotes the highest elevation of the lacustrine sediments along the Yellow River.

The dammed lake intermittently extended for −46 km upstream from the Dehenglong-Suozi landslides to Lijia Gorge along both banks of the upper Yellow River [17] (Figure 3). The lacustrine sediments consist mainly of fine sand, silt and clay, showing clear centimeter-scale bedding. Identification of the paleolake deposits is based on the lithofacies association, consisting of horizontal to subhorizontal laminated clayey-silt alternating with fine sand that buries subjacent well-rounded fluvial gravels. These lacustrine sediments were deposited post the emplacement of the dam with lake formation and lacustrine sections scattered along the upstream of the Yellow River. A weighted mean OSL age of 12 samples from Lijiaxia and Qunke sections returned ca. 80 ka for this dammed lake in our previous work [17] (Table A1 and Figure 3).

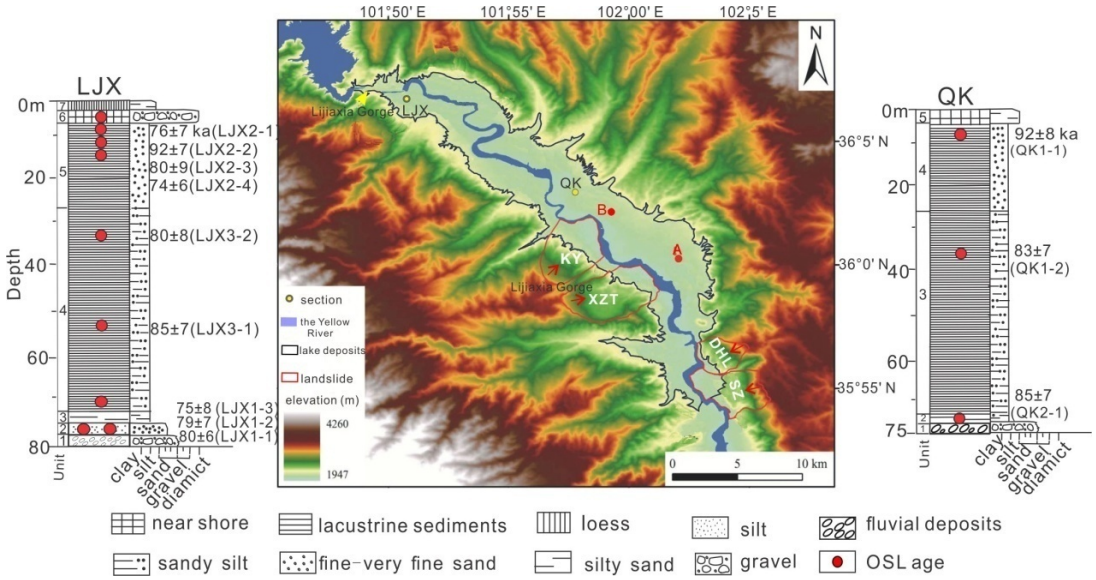

Figure 3. Digital elevation model (DEM) view for the reconstructed lake extent that is represented by the dark lines and current bed of the Yellow River is represented by blue lines. Dehenglong, Suozi, Xiazangtan and Kangyang landslides, Qunke and Lijiaxia lacustrine sediment sites are abbreviated as DHL, SZ, XZT, KY, QK, and LJX. "A" in the map denotes the outcrop where the nearshore of the dammed lake overlaid Xiazangtan landslide mass on the west bank of Xiazangtan landslide, see Figure 5A for details. "B" in the map denotes that lacustrine sediments at the front lobe of Kangyang landslide were also deformed into a series of asymmetric folds with 2–3 m amplitude, see Figure 5B for details.

The Xiazangtan and Kangyang landslides with estimated volumes of 14.18×10^8 m^3 and 14.37×10^8 m^3, emplaced ~8 km upstream of the Dehenglong–Suozi landslides (Figure 4). The basement rock, from which Xiazangtan and Kangyang landslides were detached, was Neogene red mudstone. Opposite the Xiazangtan and Kangyang landslides, on the south bank of the Yellow River, Neogene red mudstone was also observed; the same material that comprised the landslide mass on the north river bank. These geomorphic relations indicatethat Xiazangtan and Kangyang landslides were transported across the Yellow River and dammed river flow as well. Our previous geochronology work for the Dehenglong, Suozi, Xiazangtan, Kangyang landslides and dammed lake deposits revealed that these four paleolandslides emplaced penecontemporaneously at ca. 80 ka [15,18]. But it is unknown what the potential correlations are among the Dehenglong-Suozi landslides, the dammed lake deposits and these two additional landslides that occurred about 8 km upstream (Figure 1, Figure 3).

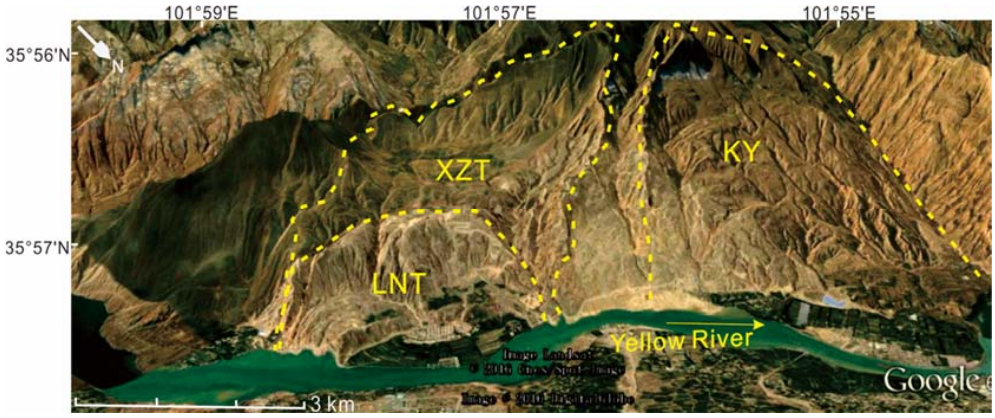

Figure 4. Google images for Xiazangtan, Kangyang and Lannitan landslides, which are abbreviated as XZT, KY and LNT.

3. Methods

3.1. Stratigraphy and Sampling

Two lacustrine sediments sections were investigated to unravel this issue in this study. (1) In an exposure on the north bank of the Yellow River, opposite Xiazangtan landslide mass, a 10 m-thick sandy-silt lake deposit buried a 20 m-thick conglomerate composed of blocks of Neogene red mudstone, the same lithology of Xiazangtan landslide on the south bank ("A" in Figure 3; see Figure 5A for details). Asymmetric folds 10 to 30 cm in amplitude were identified at the stratigraphic contact between landslide mass and lakeshore sediments (Figure 5A). The fold axes were perpendicular to the southward movement of the Xiazangtan landslide. An OSL sample XZC-1 was collected from the lens of lakeshore deposits. (2) Lacustrine sediments at the front lobe of Kangyang landslide were also deformed into a series of asymmetric folds with 2–3 m amplitude (Figure 5B). These asymmetric folds were inferred to form when Kangyang landslide slid into the dammed lake that was inundated by the Dehenglong–Suozi landslides, resulting in tsunami waves. An OSL sample(WBJ-1) was collected from silty sand.

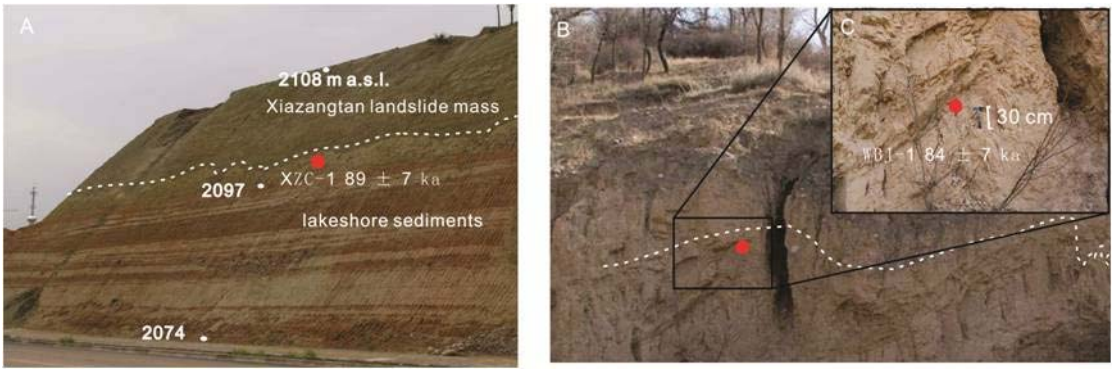

Figure 5. (**A**) The silty sand was plastically deformed with a series of asymmetric folds 20 to 40 cm in amplitude and are confined within bedding planes (36°06′58.10″ N 101°49′22.5″ E). We inferred these asymmetric folds formed when the river was dammed. (**B**) Lacustrine sediments at the front lobe of Kangyang landslide were also deformed into a series of asymmetric folds with 2–3 m amplitude. (**C**) A sample from the silty sand of the folds yielded an optical age of 84 ± 7 ka (WBJ-1).

3.2. Optically Stimulated Luminescence (OSL) Dating Method

Equivalent dose (D_e, paleodose) divided by dose rate is an optically stimulated age [34]. OSL samples were collected in opaque cores from sediments to determine their equivalent dose. The <300 μm of sediment samples were treated with 30% H_2O_2 and 10% HCl to remove organic matter and carbonate, respectively. Grains (38–63 μm) were selected by sieving and then soaked in 35% H_2SiF_6 to dissolve feldspar [35], and followed by immersion in 10% HCl acid to remove fluoride precipitates [35,36]. Infrared (IR) stimulation was used to check the purity of quartz extract. Samples that showed emissions above background counts (300 counts/s) with infrared stimulation (IRSL) were retreated with 35% $H_2SiF_6$and checked again with IRSL. Quartz grains were mounted on the center part (plate diameter 0.5–0.6 cm) of a stainless steel disc (1.0 cm in diameter) with silicone oil. The equivalent dose was determined on about 20disks for each sample with a Risø TL/OSL-DA-20 reader at the Luminescence Dating Laboratory, Qinghai Institute of Salt Lakes, Chinese Academy of Sciences. The single aliquot regenerative-dose (SAR) protocols were adopted for determining a D_e [37]. An initial pre-heat of 260°C for 10 s was used with a cut-heat of 220 °C for 10 s after a D_e dose recovery test [19].

D_e determination was obtained by combining SAR protocol [37] and standard growth curve (SGC)methods, i.e., SAR-SGC method [38,39]. Six aliquots for each sample were measured and were the basis to construct a SGC for each quartz separate. Another 10 to 14 aliquots were measured with the

same SAR procedure to determine the natural signal (L_N) and the OSL test dose (T_N). A D_e was then calculated for all the L_N/T_N data by statistical relation to the SGC. The mean and errors of the final D_e for each sample was calculated using the central age model for SAR D_es and SGC D_es. Figure 6A,B show the growth curves of individual aliquots of WBJ-1 and XZC-1, with figures showing its decay curves (Figure 6C,D). All the growth curves did not saturate and were well fitted using the exponential-linear function. All D_es determined by SGC were overlapped at one sigma errors with those by the SAR protocol. The decay curve shapes showed that OSL signal is dominated by the so called fast component, with the OSL emission decreasing by 95% during the first 4 s of stimulation (Figure 6C,D).

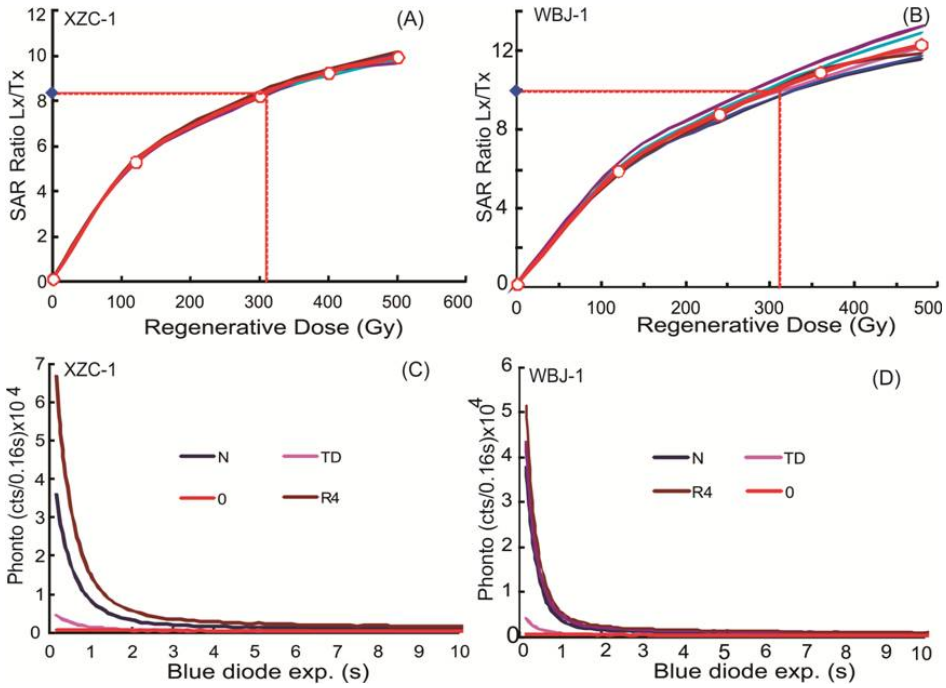

Figure 6. (**A**,**B**) showing growth curves of individual aliquots WBJ-1 and XZC-1, with basal figures showing decay curves (**C**,**D**).

A dose rate represents the rate at which energy is absorbed from the flux of nuclear radiation and is correlated with the concentrations of U, Th and K, cosmic dose rate and water content of the bulk sample. The dose rate was calculated from the concentrations of U, Th and K measured by neutron activation analysis in the China Institute of Atomic Energy in Beijing. The cosmic dose rate was estimated according to [40]. The water content of samples was assumed to be 10 ± 3% (Table 1).

Table 1. Optically stimulated luminescence (OSL) ages on quartz extracts and associated data.

Sample ID	Aliquots	Grain Size (microns)	Equivalent Dose (Gray) [c]	U (ppm) [d]	Th (ppm) [d]	K (%) [d]	H_2O (%)	Cosmic Dose (mGray/yr) [e]	Dose Rate (mGray/yr)	OSL Age (ka) [f]
WBJ-1	6 [a] + 14 [b]	38–63	273.4 ± 12.7	2.65 ± 0.14	11.3 ± 0.29	1.66 ± 0.05	10 ± 3	0.036 ± 0.002	3.25 ± 0.24	84 ± 7
XZC-1	6 [a] + 14 [b]	38–63	301.2 ± 7.0	2.51 ± 0.16	12.4 ± 0.30	2.05 ± 0.05	10 ± 3	0.167± 0.011	3.35 ± 0.24	89 ± 7

[a] aliquot number used for single aliquot regenerative-dose(SAR), [b] aliquot number used for standard growth curve(SGC), [c] Equivalent dose (D_e) analyzed under blue-light excitation (470 ± 20 nm) by single aliquot regeneration protocols [37,41]. [d] U, Th and K_2O content analyzed by neutron activation analysis in the China Institute of Atomic Energy in Beijing. [e] From Presott and Hutton [40]. [f] Systematic and random errors calculated in a quadrature at one standard deviation. Datum year is AD 2000.

3.3. Outburst Flood Calculation

A newly formed dams often induce upstream flooding as the impounded lake level rises. In turn, it may also cause downstream flooding when breached. The Dehenglong–Suozi landslides were such catastrophic dam failures they may cause huge peak discharge when breached. Large dams composed

of low shear strength material frequently fail catastrophically with release of debris flows, overtopping, and piping, and are particularly vulnerable in tectonically active areas [42,43]. The maximum potential outburst-flood was calculated with catastrophic failure of the dam for a paleo-lake assuming complete and critical flow through the breach; a reasonable approach given the relatively large water volume of the paleolake [43]. Gradual erosion of the dam or infilling of the lake with sediment could have produced lower discharge. The upper reaches of the Yellow River in Jianzha Basin currently has an average annual water discharge of 691.62 m^3/s. We estimated the breach geometry from the modern valley cross-section at the narrowest point in the valley below the landslide.

Using the Bernoulli equation for conservation for energy, h_c is the height of the water flowing through the breach, and H is the depth of the lake near the dam. We can estimate h_c from [44]:

$$h_c = H - \frac{Q^2}{2gA^2} \quad (1)$$

where Q is discharge (m^3/s), g is acceleration of gravity (9.8 m/s^2), and A is the cross-sectional area of flow (m^2).

Assuming critical flow just downstream of the breach such that the Froude number (Fr) = 1,

$$F_r = \left[\frac{Q^2 w}{gA^3}\right]^{\frac{1}{2}} = 1 \quad (2)$$

Applying Manning's equation for channel water flow capacity (Q_n),

$$Q_n = \frac{A\left(\frac{A}{P}\right)^{\frac{2}{3}} S^{\frac{1}{2}}}{n} \quad (3)$$

where P is the wetted perimeter, S is the bed slope, and n is Manning's roughness coefficient.

4. Results

4.1. Ages of Sampling

OSL sample XZC-1 collected from lens of lakeshore deposits yielded an optical age of 89 ± 7 ka at the stratigraphic contact between Xiazangtan landslide and lakeshore sediments (Figure 5A) (Table 1), which is consistent with the ages of Xiazangtan landslide and the dammed lake formed by the Dehenglong–Suozi landslides.An OSL sample from silty sand of the asymmetric folds in a lacustrine section yielded an optical age of 84 ± 7 ka (WBJ-1) at the front lobe of Kangyang landslide (Figure 5B) (Table 1), which is penecontemporaneous with the emplacing time of Kangyang landslide and the dammed lake formed by the two pairs of downstream landslides. These two OSL ages used single aliquot regeneration protocols and are younger than independently dated Chinese loess to at least 130 ka [45] and thus are finite age estimates. Therefore, the asymmetric folds at the front lobe of Kanyang landslide were inferred to form because Kangyang landslide slid into the dammed lake that was inundated by Dehenglong–Suozi landslides, resulting in tsunami waves.

4.2. Outburst Flood

Assuming the failure of the landslide dam from Google Earth: H = 180 m, A = 60,000 m^2, W = 3750 m, and combining the above Equations (1) and (2), we can iterate with the Yellow River topographic cross-section to find h_c = 176 m, and $Q = 5.6 \times 10^5 m^3/s$.

When wetted perimeter (P) is 4500 m, bed slope(S) is 0.003, and Manning's roughness coefficient (n) is 0.03–0.05, Equation (3) gives a range of Q_n of 3.7 to 6.1 × 10^5 m^3/s. This analysis suggests the channel is able to carry the critical flow (Q), at least at steady and uniform flow conditions.

5. Assessing the Landslide-Dammed Lake Volume

The lake that formed upstream of the landslide dam was also the focus of investigations (Figure 4). A digital elevation model with a resolution of 30 m was generated to estimate the lake area from digitization of a 1:50,000-scale topographic map covering the landslide and upstream areas. The landslide-dammed lake sediments intermittently extend for about 46 km upstream from the Dehenglong–Suozi landslides to Lijia Gorge and along both banks of the upper Yellow River. We inferred the highest elevation of the dam lake at 2200 m a.s.l. from the mutual highest elevation of Lijiaxia and Qunke sections. Thus, the maximum depth of the dam lake could be 180 m, combining the lowest elevation of landslide of 2020 m a.s.l. The paleolake covered an approximate area of 212.5 km^2. Therefore, a maximum estimate of lake volume was about 38 km^3, reflecting the elevational distribution of lake sediments and scattered.

There was limited accommodation space for the landslide mass because of the narrow, steep valley for this reach of the Yellow River. The extent of the landslide dam is estimated from the areal distribution of the landslide deposits on opposite banks of the Yellow River (Figure 2). The NE–SW trending remnants of the landslides mass were deposited partially on a surface that appears correlative with the fourth terrace (ca. 80 ka) along the Yellow River [30]. The lowest elevation of the landslide on the east side of the river was 2020 m a.s.l. with a run-up height of >2316 m a.s.l. on the west side of the river.

6. Discussion

6.1. Neotectonically Causative Factors for Dehenglong-Suozi Landslides

Several potential concurrent landslides were identified on the northeastern Tibetan Plateau in the past ca. 80 ka (Table 2). In Guide basin the Xijitan landslide at 80 ± 5 ka with a volume of 8.4×10^8 m^3 and Ashengong landslide at 80 ± 6 ka, with a volume of $1.6 \times 10^8 m^3$ were inferred to reflect tectonic activity of the Deqiansi-Ashengong fault (F4 in Figure 1B) [20]. All these faults are part of the Zhamashan-Wendudashi fault (F5 and F6 in Figure 1B) zone that is one of the segments of Qilian Mountain and Xiqinling Mountain massifs, both of which are still active, with a recorded earthquake of Ms 4.5 in 1958 [46]. This indicates that the Deqiansi-Ashegong fault has been active since late Pleistocene and the Dehenglong landslide is likely to be affected and propagated by these earthquakes in such a tectonically active context [22,31].

Table 2. OSL ages on quartz grains of sediments associated with landslides from Longyang Gorge to Liujia Gorge on northeast Tibetan Plateau.

Landslides	Types of Sediments	Aliquots	Grain Size (microns)	Equivalent Dose (Gray) [c]	U (ppm) [d]	Th (ppm) [d]	K (%) [d]	H_2O (%)	Cosmic Dose (uGy/kyr) [e]	Dose Rate (Gy/kyr)	OSL (ka) [f]	Age Reference
Ashegong landslide	shear zone of high friction	6 [a] + 12 [b]	38–63	323.47 ± 6.92	2.2 ± 0.1	17.5 ± 0.4	2.76 ± 0.07	15 ± 5	0.06 ± 0.04	4.05 ± 0.29	80 ± 6	[20]
Dehenglong landslide	swale deposits on landslid (loess)	6 [a] + 14 [b]	38–63	355.7 ± 19.1	2.2 ± 0.1	17.5 ± 0.4	2.88 ± 0.05	10 ± 5	0.01 ± 0.001	3.75 ± 0.26	89 ± 8	[16]
Dehenglong fault	fault gauge	6 [a] + 14 [b]	38–63	378.9 ± 8.0	11 ± 0.3	9.6 ± 0.3	2.13 ± 0.06	10 ± 5	0.01 ± 0.001	4.83 ± 0.33	73 ± 5	[16]
Suozi landslide	Shear zone of high friction (Trassic gneiss)	6 [a] + 14 [b]	38–63	265.8 ± 10.1	2.4 ± 0.1	10.9 ± 0.3	2.09 ± 0.06	5 ± 5	0.19± 0.01	3.3 ± 0.23	71 ± 6	[15]
Xiazangtan landslide	swale deposits on landslide (loess)	6 [a] + 14 [b]	38–63	232.08 ± 9.83	2.9 ± 0.2	13.6 ± 0.3	1.48 ± 0.05	10 ±3	0.02 ± 0.001	3.11 ± 0.17	75 ± 9	[18]
Kangyang landslide	loess overlying the landslide	6 [a] + 12 [b]	38–63	110.41 ± 5.53	5.4 ± 0.2	10.4 ± 0.3	1.90 ± 0.06	10 ± 3	0.27 ± 0.03	3.89 ± 0.27	28 ± 2	[18]
	terrace overlain the landslide	6 [a] + 14 [b]	38–63	187.45±10.21	2.7 ± 0.1	10.4 ± 0.2	1.64 ± 0.06	10 ± 3	0.15 ± 0.01	3.16 ± 0.17	86 ± 6	[18]
										Mean & SD	79 ± 9	
Maijia landslide	loess overlying the landslide	6 [a] + 12 [b]	38–63	171.60 ± 5.25	3.0 ± 0.2	11.3 ± 0.3	1.85 ± 0.06	15 ± 5	0.27 ± 0.03	3.89 ± 0.27	49 ± 3	[23]
Jishixia landslide	swale deposits on landslide (loess)	6 [a] + 12 [b]	38–63	128.27 ± 1.85	1.9 ± 0.1	9.5 ± 0.3	2.04 ± 0.07	15 ± 5	0.21 ± 0.01	3.03 ± 0.22	42 ± 3	[23]
Tangse landslide	shear zone of high friction	6 [a] + 12 [b]	38–63	138.06 ± 2.35	4.2 ± 0.2	12.5 ± 0.3	269 ± 0.07	15 ± 5	0.07 ± 0.01	4.19 ± 0.30	33 ± 2	[20]
Tangjiashan landslide	shear zone of high friction	6 [a] + 12 [b]	38–63	461.79 ± 9.25	3.9 ± 0.2	11.1 ± 0.3	2.15 ± 0.06	15 ± 5	0.17 ± 0.01	3.63 ± 0.25	127 ± 9	[23]

[a] aliquot number used for SAR, [b] aliquot number used for SGC. [c] Equivalent dose (D_e) analyzed under blue-light excitation (470 ± 20 nm) by single aliquot regeneration protocols [37,41]. [d] U, Th and K_2O content analyzed by neutron activation analysis in China Institute of Atomic Energy in Beijing. [e] FromPresott and Hutton [40]. [f] Systematic and random errors calculated in a quadrature at one standard deviation. Datum year is AD 2000.

At the confluence of the Wendudasi Fault (F6 in Figure 1B) and the Yellow River, the active channel abruptly turns east, with the Dehenglong–Suozi landslides to the northeast of this fault. The head scarps of the Dehenglong–Suozi landslide appear to originate near the Jianzhadong Fault (255°∠48°, strike and dip of fault plane) (F9 in Figure 1B). Whereas, the Dehenglong Fault (75°∠65°) displaces the front lobe of the landslides (F8 in Figure 1B) [22]. The Dehenglong Fault upthrusted Neogene red mudstone and late Triassic gneiss where the fault breccia's yielded an OSL age on quartz grains of 73 ± 5 ka (F8 in Figure 1B, Table 1) [16], which appears to be in accordance with the age of the dammed lake sediments. Neogene red mudstone, similar material that composed the landslide mass on the north bank, overlies massive gravel and horizontal laminated medium sands, which displaced fluvial sediment. This stratigraphic contact was inferred to be associated with the movement of the Dehenglong landslide across the Yellow River with sufficient velocity to have deformed and, in places, overturned fluvial deposits [16]. Quartz grains from an overturned fluvial sand yielded an OSL age of 74 ± 8 ka [16], which is consistent with OSL ages (at 2 sigma errors) of the Suozi landslide (71 ± 6 ka) and Dehenglong landslide (89 ± 8 ka). Hence, there is a consistent chronology, at two sigma errors, for Dehenglong landslide (89 ± 8 ka) and Suozi landslide (71 ± 6 ka), and activity of Dehenglong fault (73 ± 5 ka) and associated landslide-dammed lake deposits (ca. 80 ka) which may indicate that the initiation of the Dehenglong–Suozi landslides was associated closely with displacement of Dehonglong Fault [16].

6.2. Geomorphic Effects of Landslides' Dam Upstream

The presence of one or several landslide dams increases significantly the response time of a basin to external perturbations [47]. There are numerous examples of late Pleistocene and Holocene rockslide dams in the Himalayas, the Tien Shan Mountains, and the Southern Alps of New Zealand, which formed persistent ($\leq 10^4$ year) knickpoints and sediment reservoirs in the river channel [10]. What formed post the emplacements of Dehenglong and Suozi landslides was a 46 km-long up-river lake, a large and prolonged (10^3 to10^4 year timescale) river-blocking event. Development of this 46 km-long lake behind the Dehenglong–Suozi landslides, was inferred to raise eventually the local water table, and saturated slope sediments between 80 and 170 m above the present valley floor that is associated with the tread of Terrace 4 dated at ca. 80 ka [48] (Figure 7). However, Xiazangtan and Kangyang landslides are about 8 km upstream from Dehenglong-Suozi landslides and within the range of the dammed lake. It has been reported that downstream of the blockage, backwater inundating the valley floor as a dammed lake formed may increase pore water pressure, consequently induce secondary slope failures with the risk of displacement waves [24]. Two lacustrine sediments sections have been investigated to explore whether the failures of Xiazangtan and Kangyang landslides was correlated with the downstream blockage caused by the Dehenglong–Suozi landslides. Firstly, folds were deformed at the bedding panel between silty lacustrine sediment and landslide mass and are perpendicular to the southward movement of the Xiazangtan landslide (Figure 5A). Secondly, asymmetric folds in the lacustrine sediments were deformed at the front lobe of Kangyang landslide as well (Figure 5B). These two deformed folds returned optical ages of 89 ± 7 ka (XZC-1) and 84 ± 7 ka (WBJ-1) respectively, which were consistent with the ages of the Dehenglong–Suozi landslides (89 ± 8 and 71 ± 6 ka), Xiazangtan-Kangyang landslides (75 ± 9 ka and 33–85 ka) and lake deposits and Dehenglong fault (ca. 80 ka) at two sigma errors.

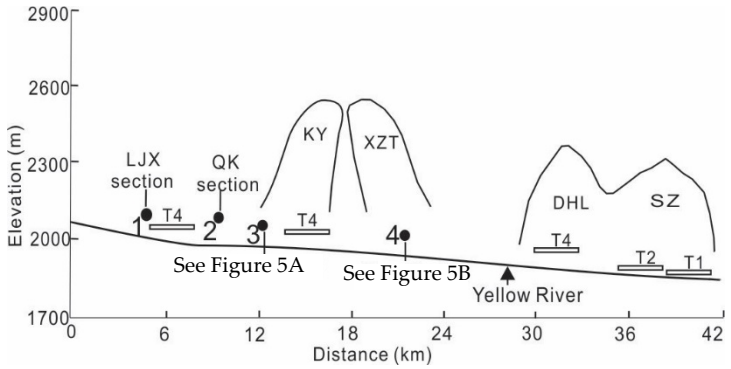

Figure 7. Longitudinal river profile showing present-day elevation, locations of landslides, terraces and lacustrine sediments. "3" denotes an outcrop where nearshore of the dammed lake overlaid the Xiazangtan landslide mass on the west bank of the Yellow River. "4" denotes folds in the lacustrine sediments at the toe of Kangyang landslide, which is inferred to reflect that the dammed lake caused by the Dehenglong–Suozi landslides was surged to the north bank of the Yellow River. T1, T2 and T4 denote the first, second and fourth terrace. The third terrace was inferred to be eroded in to and/or capped by landslide deposits and lake sediments.

This cluster of four landslides adjacent to the Yellow River that occurred ca. 80 ka (Table 1) may reflect a number of processes. The Dehenglong–Suozi landslides emplaced firstly and dammed the Yellow River because that Dehenglong fault upthrusted the front lobe of Dehenglong landslide. The emplacement of the initial Dehenglong–Suozi landslides downstream further raised the adjacent lake table, water saturating sediments and reducing shear strength, eventually induced the other two subsequent landslides (Xiazangtan and Kangyang) within the paleo-lake basin that occurred between ca. 80 ka, as assessed through OSL dating.

6.3. Disasters of Subsequent Outburst Flood Downstream

Examples of breached outburst flood are common in the world, such as the Sitna River Basin [49] and upper Tisa Basin [50], Romania and Vietnam [51]. The Yellow River, the second longest river in China, is a major source of freshwater for about 107 million people within this river basin in northern China. An outburst flood, with a peak discharge of 3.5×10^5 m^3/s, from a dammed lake that formed due to an earthquake-triggered paleo-landslide destroyed the Qijia settlement near the Lajia site at 4270–3850 cal yr BP in Guantin Basin that is adjacent to our study area [14]. A flood from the dammed lake formed by the Dehenglong–Suozi landslides with a magnitude of 6.1×10^5 m^3/s, would incorporate a significant amount of easily eroded sediment, including boulders and would develop into debris deluge, many times the volume of the flow emanating from the breach in the dam. The breach of this dammed lake would bring about devastating disasters to Jianzha County, with a population of 54,000 situated on the main mass of the Dehenglong–Suozi paleo-landslides on the south bank of the Yellow River and Xunhua County, with a recent population of approximately 126,000.

The Dehenglong and Xiazangtan landslide masses are also contemporary sources for landslides because of the low shear strength of previous deposited material at a high internal angle >20°. Remotely sensed observations and field investigation indicate that the Xiazangtan landslide has been reactivated three times since its emplacement ca. 80 ka. As a case-in-point, the Lannitan landslide occurred on 19 August 2005 with a volume of 14.18×10^8 m^3 (Figure 4); a secondary reactivation event from the toe of Xiazangtan landslide, caused damage to buildings, destroyed cables, blocked roads, and buried farmlands, although with pre-warning there were few injuries. The existing landslide masses may reactivate or a new landslide may occur, again damming the Yellow River, which reflects multiple overlapping processes related to regional hydrology, fluvial erosional thresholds and tectonic activity.

7. Conclusions

It was proposed in a previous study that two pairs of paleolandslides, Dehenglong–Suozi and Xiazangtan-Kangyang, 8 km-away, dammed the Yellow River at ca. 80 ka and formed a 46 km-long lake stretching up the River on the northeastern Tibetan Plateau. This study focused on the trigger factors for these four landslides and correlations between these two pairs of paleolandslides. Earthquake events from nearby capable faults may have been a contributing factor for the Dehenglong–Suozi landslides, particularly during periods of aggradation and high water tables along the steep upper reaches of the Yellow River. Deformed folds in the lakeshore or lacustrine sediment sections that are opposite the Xiazangtan landslide and at the front lobe of the Kangyang landslide, returned 89 ± 7 ka (XZC-1) and 84 ± 7 ka (WBJ-1), respectively. Thus, we inferred that a rise in lake water, lowered shear stress for adjacent sediment as the formation of the landslide-dammed lake appeared to have induced the additional two landslides (Xiazangtan and Kangyang) within the paleo-lake basin that occurred at ca. 80 ka, as assessed through OSL dating. The landslide dammed lake resulted in the upstream impoundment of water and sediment with an estimated volume of 38 km^3. A catastrophic breach of this dam may have generated an outburst flood with an estimated peak discharge of 6.1 $\times 10^5$ m^3/s.

Author Contributions: Conceptualization, Writing—original draft and Funding acquisition, X.G.; Formal analysis, Y.L. and X.G.; Investigation, X.G.; J.W. and Z.S.; Methodology, H.L. All authors have read and agreed to the published version of the manuscript.

Funding: This study was funded by the China Postdoctoral Science Foundation Funded Project Grant, No. 2019M652430, 01020240307, 201903028.

Conflicts of Interest: The authors declare no conflict of interest.

Appendix A

Table A1. OSL ages on quartz extracts and associated data of lacustrine sediments from our previous work [17].

Sample ID	Grain Size		Equivalent	U	Th	K	H_2O	Cosmic Dose	Dose Rate	OSL Age
	Aliquots	(microns)	Dose (Gray) [c]	(ppm) [d]	(ppm) [d]	(%) [d]	(%)	(mGray/yr) [e]	(mGray/yr)	(ka) [f]
LJX1-1	6 [a] + 14 [b]	38–63	265.6 ± 8.4	3.12 ± 0.14	12.12 ± 0.33	1.77 ± 0.05	10 ± 3	0.006 ± 0.000	3.08 ± 0.22	80 ± 6
LJX1-2	6 [a] + 14 [b]	38–63	259.5 ± 14.4	2.67 ± 0.17	11.20 ± 0.28	1.93 ± 0.06	10 ± 3	0.032 ± 0.002	3.10 ± 0.22	79 ± 7
LJX1-3	6 [a] + 14 [b]	38–63	225.1 ± 17.8	2.65 ± 0.15	10.0 ± 0.05	1.70 ± 0.06	10 ± 3	0.150 ± 0.050	2.80 ± 0.21	75 ± 8
LJX2-1	6 [a] + 14 [b]	38–63	198.3 ± 9.9	1.46 ± 0.11	9.4 ± 0.27	1.56 ± 0.05	10 ± 3	0.071± 0.005	2.43 ± 0.18	76 ± 7
LJX2-2	6 [a] + 14 [b]	38–63	250.9 ± 10.7	1.68 ± 0.11	9.64 ± 0.25	1.65 ± 0.05	10 ± 3	0.058 ± 0.004	2.55 ± 0.19	92 ± 7
LJX2-3	6 [a] + 14 [b]	38–63	229.3 ± 6.9	2.4 ± 0.14	9.64 ± 0.28	1.62 ± 0.06	10 ± 3	0.150 ± 0.050	2.65 ± 0.19	80 ± 9
LJX2-4	6 [a] + 14 [b]	38–63	232.9 ± 9.8	3.7 ± 0.17	8.59 ± 0.23	1.73 ± 0.06	10 ± 3	0.150 ±0.050	2.95 ± 0.21	74 ± 6
LJX3-1	6 [a] + 14 [b]	38–63	219.4 ± 8.9	1.97 ± 0.12	8.96 ± 0.25	1.48 ± 0.05	10 ± 3	0.150 ± 0.050	2.40 ± 0.18	85 ± 7
LJX3-2	6 [a] + 14 [b]	38–63	222.1 ± 14.9	1.97 ± 0.12	8.88 ± 0.25	1.67 ± 0.05	10 ± 3	0.150 ± 0.050	2.60 ± 0.19	80 ± 8
QK1-1	6 [a] + 14 [b]	38–63	244.5 ± 9.7	2.22 ± 0.13	9.89 ± 0.27	1.47 ± 0.05	10 ± 3	0.150 ± 0.050	2.47 ± 0.18	92 ± 8
QK1-2	6 [a] + 14 [b]	38–63	240.1 ± 10.5	2.24 ± 0.13	11.1 ± 0.31	1.66 ± 0.05	10 ± 3	0.150 ± 0.050	2.71 ± 0.20	83 ± 7

[a] Aliquot number used for SAR. [b] Aliquot number used for SGC. [c] Equivalent dose (D_e) analyzed under blue-light excitation (470 ± 20 nm) by single aliquot regeneration protocols [37,41]. [d] U, Th and K_2O content analyzed by neutron activation analysis in China Institute of Atomic Energy in Beijing. [e] From Presott and Hutton [40]. [f] Systematic and random errors calculated in a quadrature at one standard deviation. Datum year is AD 2000.

References

1. Korup, O.; Montgomery, D.R. Tibetan plateau river incision inhibited by glacial stabilizationof the Tsangpo gorge. *Nature* **2008**, *455*, 786–789. [CrossRef]
2. Dai, F.C.; Lee, C.F.; Deng, J.H.; Tham, L.G. The 1786 earthquake-triggered landslide dam and subsequent dam-break flood on the Dadu River, southwestern China. *Geomorphology* **2005**, *65*, 205–221. [CrossRef]
3. O'connor, J.E.; Costa, J.E. *The World's Largest Floods, Past and Present: Their Causes and Magnitudes*; Geological Survey (USGS): Reston, VA, USA, 2004; p. 1254.

4. Wang, H.J.; Yang, Z.S.; Saito, Y.; Liu, J.P.; Sun, X.X. Interannual and seasonal variation of the Huanghe (Yellow River) water discharge over the past 50 years: Connections to impacts from ENSO events and dams. *Glob. Planet. Chang.* **2006**, *50*, 212–225. [CrossRef]
5. Wang, Y.; Herzschuh, U.; Liu, X.; Korup, O.; Diekmann, B. A high-resolution sedimentary archive from landslide-dammed Lake Mengda, north-eastern Tibetan Plateau. *J. Paleolimnol.* **2012**, *51*, 303–312. [CrossRef]
6. Wang, P.; Chen, J.; Dai, F.; Long, W.; Xu, C.; Sun, J.; Cui, Z. Chronology of relict lake deposits around the Suwalong paleolandslide in the upper Jinsha River, SE Tibetan Plateau: Implications to Holocene tectonic perturbations. *Geomorphology* **2014**, *217*, 193–203. [CrossRef]
7. Chen, Y.Z. Investigation the Flood History of the Yellow River: From Analyzing Historical Records to Computer Modeling. Ph.D. Thesis, Nanjing University, Nanjing, China, 2006. (In Chinese with English abstract).
8. Liu, W.; Lai, Z.; Hu, K.; Ge, Y.; Cui, P.; Zhang, X.; Liu, F. Age and extent of a giant glacial-dammed lake at Yarlung Tsangpo gorge in the Tibetan Plateau. *Geomorphology* **2015**, *246*, 370–376. [CrossRef]
9. Zhang, Y.; Huang, C.C.; Shulmeister, J.; Guo, Y.; Liu, T.; Kemp, J.; Patton, N.R.; Liu, L.; Chen, Y.; Zhou, Q.; et al. Formation and evolution of the Holocene massive landslide-dammed lakes in the Jishixia Gorges along the upper Yellow River: No relation to China's Great Flood and the Xia Dynasty. *Quat. Sci. Rev.* **2019**, *218*, 267–280.
10. Korup, O. Effects of large deep-seated landslides on hillslope morphology, western Southern Alps, New Zealand. *J. Geophys. Res. Earth Surfaces* **2006**, *111*. [CrossRef]
11. Ouimet, W.B.; Whipple, K.; Royden, L.; Sun, Z.; Chen, Z. The influence of large landslides on river incision in a transient landscape: Eastern margin of the Tibetan Plateau (Sichuan, China). *Geol. Soc. Am. Bull.* **2007**, *119*, 1462–1476. [CrossRef]
12. Restrepo, C.; Walker, L.R.; Shiel, A.B.; Bussmann, R.; Claessens, L.; Fisch, S.; Lozano, P.; Negi, G.; Paolini, L.; Poveda, G.; et al. Landsliding and its multiscale influence on mountainscapes. *Bioscience* **2009**, *59*, 685–698. [CrossRef]
13. Mackey, B.H.; Roering, J.J.; Lamb, M.P. Landslide-dammed paleolake perturbs marine sedimentation and drives genetic change in anadromous fish. *Proc. Natl. Acad. Sci. USA* **2011**, *108*, 18905–18909. [CrossRef]
14. Wu, Q.; Zhao, Z.; Liu, L.; Granger, D.E.; Wang, H.; Cohen, D.J.; Wu, X.; Ye, M.; Yosef, O.; Lu, B.; et al. Outburst flood at 1920 BCE supports historicity of China's Great Flood and the Xia dynasty. *Science* **2016**, *353*, 579–582. [CrossRef]
15. Guo, X.; Lai, Z.; Sun, Z.; Li, X.; Yang, T. Luminescence dating of Suozi landslide in the Upper Yellow River of the Qinghai-Tibetan Plateau, China. *Quat. Int.* **2014**, *349*, 159–166. [CrossRef]
16. Guo, X.; Lai, Z.; Lu, Y.; Li, X.; Sun, Z. Optically Stimulated Luminescence (OSL) Chronology of the Dehenglong Landslide from Longyang Gorge to Liujia Gorge along Upper YellowRiver. *Acta Geol. Sin. Engl. Ed.* **2015**, *89*, 242–250.
17. Guo, X.; Sun, Z.; Lai, Z.; Lu, Y.; Li, X. Optical dating of landslide-dammed lake deposits in the upper Yellow River, Qinghai-Tibetan Plateau, China. *Quat. Int.* **2016**, *392*, 233–238. [CrossRef]
18. Guo, X.H. OSL Chronology of Giant Landslides from Longyangxia Gorge to Liujia Gorge Along Upper Yellow River. Master's Thesis, Lanzhou University, Lanzhou, China, 2012. (in Chinese with English Abstract).
19. Guo, X.; Wei, J.; Song, Z.; Lai, Z.; Yu, L. Optically stimulated luminescence chronology and geomorphic imprint of Xiazangtan landslide upon the upper Yellow River valley on the northeastern Tibetan Plateau. *Geol. J.* **2020**. [CrossRef]
20. Zhou, B. Research on Development Characteristic and Mass Mechanism of Super Large Landslide in the Upper Yellow River. Ph.D. Thesis, Chang'an University, Xi'an, China, 2011.
21. Zhou, B.; Hu, G.S.; Peng, J.B.; Lu, B.C. An evaluation on the basis of GIS of risk for landslides from Laganxia Gorge to Sigouxia Gorge. *South North Water Transf. Water Sci. Technol.* **2010**, *8*, 36–48, (In Chinese with English abstract).
22. Li, X.; Guo, X.; Li, W. Mechanism of giant landslides from longyangxia valley to Liujiaxia valley along upper Yellow River. *J. Eng. Geol.* **2011**, *19*, 516–529.
23. Zhao, R.; Zhou, B. The application of optical stimulate luminescence dating to the study of clustered landslides activity. *Geol. Bull. Chin.* **2013**, *32*, 26–34, (In Chinese with English abstract).
24. Higgitt, D.; Zhang, X.B.; Liu, W.M.; Tang, Q.; He, X.B.; Ferrant, S. Giant palaeo-landslide dammed the Yangtze river. *Geosci. Lett.* **2014**, *1*, 6. [CrossRef]

25. Evans, S.G. The maximum discharge of outburst floods caused by the breaching of man-made and natural dams. *Can. Geotech.J.* **1986**, *23*, 385–387. [CrossRef]
26. Korup, O.; Clague, J.J.; Hermanns, R.L.; Hewitt, K.; Strom, A.L.; Weidinger, J.T. Giant n landslides, topography, and erosion. *Earth Planet. Sci. Lett.* **2007**, *261*, 578–589. [CrossRef]
27. Dibiase, R.A.; Whipple, K.X. The influence of erosion thresholds and runoff variability on the relationships among topography, climate, and erosion rate. *J. Geo Res.: Earth Surface* **2011**, *116*. [CrossRef]
28. Langston, A.L.; Temme, A.J.A.M. Bedrock erosion and changes in bed sediment lithology in response to an extreme flood event: The 2013 Colorado Front Range flood. *Geomorphology* **2019**, *328*, 1–14. [CrossRef]
29. Li, J. The environmental effects of the uplift of the Qinghai-Xizang Plateau. *Quat. Sci. Rev.* **1991**, *10*, 479–483.
30. Zhao, Z.; Liu, B. Relation between the formation of the Yellow River valley landforms from Gonghe, Qinghai to Lanzhou, Gansu and the uplifting in northeast part of Qinghai-Xizang plateau. *Northwest. Geol.* **2003**, *36*, 1–12.
31. Craddock, W.; Kirby, E.; Harkins, N.W.; Zhang, H.; Shi, X.; Liu, J. Rapid fluvial incision along the Yellow River during headward basin integration. *Nat. Geosci.* **2010**, *3*, 209–213. [CrossRef]
32. Li, W.; Dong, Y.; Guo, A.; Liu, X.; Zhou, D. Chronology and tectonic significance of Cenozoic faults in the Liupanshan Arcuate Tectonic Belt at the northeastern margin of the Qinghai–Tibet Plateau. *J. Asian Earth Sci.* **2013**, *73*, 103–113. [CrossRef]
33. Guo, X.; Lu, Y.D.; Li, X.L.; Sun, Z.; Li, C.Y.; Zhang, R. Event of Block up upper Yellow River by Dehenglong-Suozi landslides. *J. Jilin Univ. Earth Sci. Ed.* **2015**, *45*, 1789–1797.
34. Aitken, M.J. *Introduction to Optical Dating: The Dating of Quaternary Sediments by the Use of Photon-Stimulated Luminescence*; Oxford University Press: New York, NY, USA, 1998.
35. Lai, Z. Chronology and the upper dating limit for loess samples from Luochuan section in the Chinese Loess Plateau using quartz OSL SAR protocol. *J. Asian Earth Sci.* **2010**, *37*, 176–185. [CrossRef]
36. Lai, Z.P.; Wintle, A.G. Locating the boundary between the Pleistocene and the Holocene in Chinese loess using luminescence. *Holocene* **2006**, *16*, 893–899. [CrossRef]
37. Murray, A.S.; Wintle, A.G. The single aliquot regenerative dose protocol: Potential for improvements in reliability. *Radiat. Meas.* **2003**, *37*, 377–381. [CrossRef]
38. Roberts, H.M.; Duller, G.A.T. Standardized growth curves for optical dating of sediment using multiple-grain aliquots. *Radiat. Meas.* **2004**, *38*, 241–252. [CrossRef]
39. Lai, Z.P.; Brückner, H.; Zöllerb, F.A. Existence of a common growth curve for silt-sized quartz OSL of loess from different continents. *Radiat. Meas.* **2007**, *42*, 1432–1440. [CrossRef]
40. Prescott, J.R.; Hutton, J.T. Cosmic ray contributions to dose rates for luminescence and ESR dating: Large depths and long-term time variations. *Radiat. Meas.* **1994**, *23*, 497–500. [CrossRef]
41. Wintle, A.G.; Murray, A.S. A review of quartz optically stimulated luminescence characteristics and their relevance in single-aliquot regeneration dating protocols. *Radiat. Meas.* **2006**, *41*, 369–391. [CrossRef]
42. Costa, J.E.; Schuster, R.L. The formation and failure of natural dams. *Geol. Soc. Am. Bull.* **1998**, *100*, 1054–1068. [CrossRef]
43. Connor, J.E.; Beebee, R.A. *Floods from natural rock-material dams. Megaflooding on Earth, Mars*; Cambridge University Press: New York, NY, USA, 2009; pp. 128–163.
44. Chow, V.T. *Open-Channel Hydraulics*; McGraw-Hill: New York, NY, USA, 1959; pp. 40–59.
45. Lu, Y.C.; Wang, X.L.; Wintle, A.G. A new OSL chronology for dust accumulation in the last 130,000 year for the Chinese Loess Plateau. *Quart. Res.* **2007**, *67*, 152–160. [CrossRef]
46. Lv, B.C. *Report on Validation for Basically Seismic Intensity and Risk for Engineering Earthquakes in Lijia Power Station along Yellow River*; Qinghai University Press: Xining, China, 1989.
47. Korup, O.; Densmore, A.L.; Schlunegger, F. The role of landslides in mountain range evolution. *Geomorphology* **2010**, *120*, 77–90. [CrossRef]
48. Guo, X.; Forman, S.L.; Marin, L.; Li, X. Assessing tectonic and climatic controls for Late Quaternary fluvial terraces in Guide, Jianzha, and Xunhua Basins along the Yellow River on the northeastern Tibetan Plateau. *Quat. Sci. Rev.* **2018**, *195*, 109–121. [CrossRef]
49. Albu, L.M.; Enea, A.; Toleriu, C.C.S.; Niacsu, L.G.I.S. Implementation on Dam-Break Flood Vulnerability Analysis—A Case Study of Cătămărăști Dam, Botoșani, Romania. In Proceedings of the Air and Water-Components of the Environment, Cluj-Napoca, Romania, July 2019; pp. 65–75. [CrossRef]

50. Macklin, M.; Brewer, P.; Balteanu, D.; Coulthard, T.; Driga, B.; Howard, A.; Zaharia, S. The long-term fate and environmental significance of contaminant metals released by the January and March 2000 mining tailings dam failures in Maramureș County, upper Tisa Basin, Romania. *Appl. Geochem.* **2003**, *18*, 241–257. [CrossRef]
51. Luo, P.; Mu, D.; Xue, H.; Ngo-Duc, T.; Dang-Dinh, K.; Takara, K.; Nover, D. Geoffrey Schladow, Flood inundation assessment for the Hanoi Central Area, Vietnam under historical and extreme rainfall conditions. *Sci. Rep.* **2018**, *8*, 1–11. [CrossRef] [PubMed]